

Physical Modeling of Graphene Nanoribbon FET- Quantum Mechanics

Nanda B.S Puttaswamy P.S



Abstract—limited by scaling challenges of CMOS devices, the option to improve device performance is to look for novel materials and devices. Carbon, Carbon nanotubes (CNT) and graphene are prominent contenders for substituting silicon in near future. Graphene nanoribbon (GNR) which share many of the fascinating electrical and mechanical properties of CNT are a suitable device material because of compatibility with lithography process. A double gate GNR-FET is simulated by solving quantum transport equation with self-consistent electrostatics, while incorporating non-parabolic band structure of GNR-FET. Non equilibrium Green's function (NEGF) approach is used for device simulation. This paper provides physical modeling of GNR-FET and investigates the device characteristics and performance for different families of GNRs as well as for different GNR widths.

Index Terms—scaling, CNT, graphene, GNR, NEGF

I. INTRODUCTION

Scaling down of transistor dimensions has for decades enhanced the device performance and density and has been the driving engine for the exponential growth of processor systems. However, the scaling challenges in silicon based CMOS devices is limiting the further improvements and ITRS has already stated the end of Moore's law in few years. To further improve upon the device performance, the options available are to look for novel materials and devices for integrated circuits. With scaling limit in sight, a large group of emerging materials and devices are extensively being studied to replace silicon [1] especially Germanium and Carbon. Among the allotropes of Carbon, carbon nanotubes (CNT) and graphene have become prominent contenders to substitute silicon in post-CMOS technologies [2-4].

Graphene is one atomic layer of carbon sheet in a honeycomb lattice and can outperform state of the art silicon in many applications [5,6] due to its exceptional carrier mobility, high carrier concentration, high thermal conductivity and thin planar structure. The carrier transport in graphene is similar to massless particle providing high carrier velocity and high carrier concentration.

Revised Manuscript Received on January 30, 2020.

* Correspondence Author

Nanda B.S*, Department of Electronics & Communication Engineering, P E S College of Engineering, India.

Puttaswamy P.S, Department of Electrical & Electronics Engineering P E S College of Engineering, India.

© The Authors. Published by Blue Eyes Intelligence Engineering and Sciences Publication (BEIESP). This is an [open access](https://creativecommons.org/licenses/by-nc-nd/4.0/) article under the CC-BY-NC-ND license <http://creativecommons.org/licenses/by-nc-nd/4.0/>

While highly packed silicon devices suffer from removal of dissipated heat, the excellent thermal conductivity of graphene provides a convenient alternative. Atomically thin monolayer of graphene provides a better gate control over the channel and the planar structure is compatible with current CMOS fabrication process, a potential for wafer scale production [7]. Lack of bandgap in large area graphene limits the use for integrated circuits and hence only narrow stripes of graphene called graphene nanoribbon (GNR) are required. GNRs can be fabricated from large area graphene using high resolution e-beam lithography. GNRs share many of the fascinating electrical, mechanical and thermal properties of CNT. The mean free path of electrons in GNRs with smooth edge is comparable to CNT and GNR have a very large current conduction capacity with extraordinary mechanical strength and thermal conductivity. The progress in fabrication of Graphene nanoribbon is accompanied with substantial achievements in the theoretical work based on analytical approaches and numerical simulation techniques for the modeling of GNRs. Three approaches based on classical, semi-classical and quantum mechanics can be used in the study of transport phenomenon in graphene devices. The classical approach like the charge-collection equations [8] or the drift-diffusion equations are based on Newton's laws and can be employed to model large dimensions and are not very suitable for the sub-nanometer channel lengths. For the graphene nanoribbon FET with the channel lengths <10nm the mean free path can be only a few micro meters and the carrier transport can be interpreted as ballistic motion. Figure 1 shows the scaling of channel length can result in a significant direct source to drain tunneling and band to band tunneling from drain to channel. As the direct carrier tunneling from source to drain regions becomes prominent component in the drain to source current, the semi-classical models cannot be used and quantum based models [9,10] need to be considered which can take into account tunneling effects in short channel GNR-FET.

Quantum based simulation is most computationally demanding approach. The most accurate quantum based method for bottom-up device simulation is the Non-Equilibrium Green's function (NEGF) approach. In this approach, the Schrodinger equation is solved under non-equilibrium condition. The NEGF formalism provides atomistic description of channel, contacts and scattering on carrier transport in the channel. The device Hamiltonian can be discretized providing two alternative approaches for NEGF formalism: real space formalism [11] which can be used directly for any geometry and mode space formulation [12] which splits up the device simulation into set of 1D problems over the sub-bands.



Mode Space approach can be applied for simulating nanometer channel materials such as carbon nanotube [13, 14], silicon MOSFET [15] and graphene nanoribbon [16, 17]. Ouyang *et al.* [9] studied the scaling behavior of GNRFETs below 10nm considering only one family of armchair GNRs. GNRFET performance with variations in channel width was studied by Kliros [18].

The present work develops a full quantum transport model based on NEGF formalism for a Graphene Nanoribbon FET with a double gate high k-dielectric materials in order to reduce the short channel effects and reduce the leakage current. The width dependent performance of GNRFET is discussed in detail. The paper is organized as follows. Section II discusses the NEGF formulation for the carrier transport and simulations for the proposed device. In Section III, results related to width dependent performance of GNRFET are discussed while Section IV presents the conclusions.

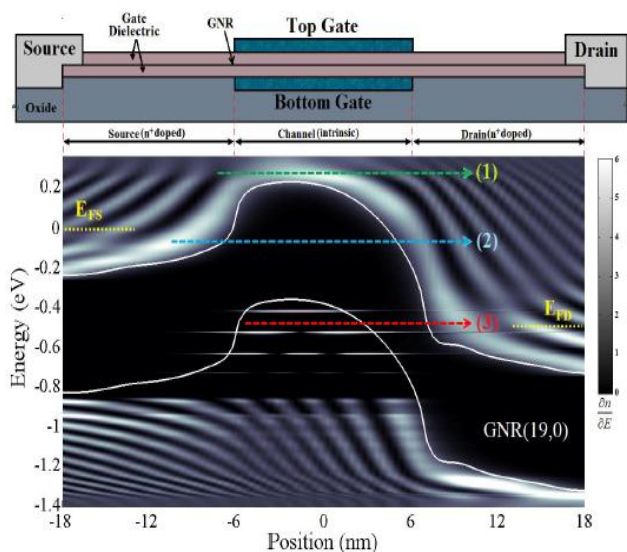


Figure 1: Carrier Transport in GNRFET

II. MODELING OF GNRFET DEVICE

Quantum based transport simulation approach is computationally most efficient approach as the device length scales down and quantum effects become more and more significant. The most accurate of these methods is the NEGF approach providing atomistic description of channel material as well as the effects of contacts on carrier transport in the channel which provides an accurate result and insight into the GNRFET performance for channel lengths < 10nm. The mode space approach of NEGF formulation when applied to the GNRFET with the assumption of smooth edges and negligible potential variation, results in a considerable computational advantage without compromising the simulation accuracy. Figure 2 & Figure 5 shows the iterative algorithm for calculating potential profile using electrostatic and transport solutions. Before obtaining the bias current, the potential profile and the charge density needs to be calculated using the Poisson's equation and the transport equation. The total charge density is obtained by summing the electron and hole densities in the channel.

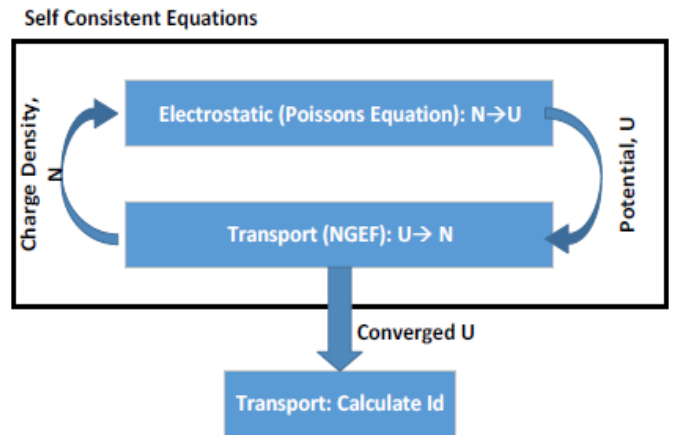


Figure 2: Self consistent electrostatic & transport computations

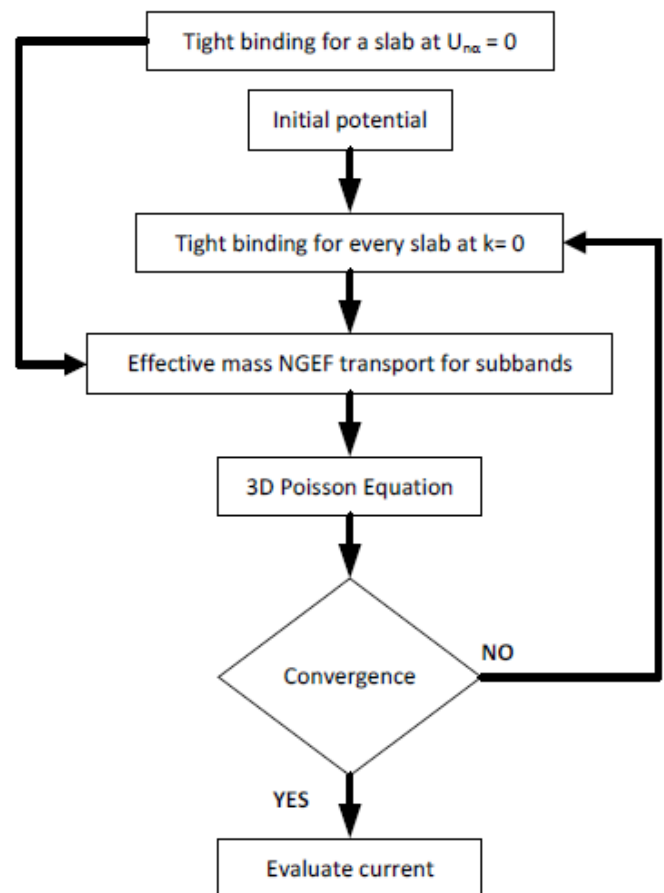


Figure 3: Iterative solution flowchart

The steps of calculating the bias current are described below.

- Step1:** Using tight binding (TB) calculation, the effective masses of the lowest sub-bands are extracted for a given width and a slab with zero potential. This shall be used in the successive transport calculations. Calculating Tight Binding inside the slabs with length of $3a_{cc}$ and $2N_a$ atoms provides the required information of GNR sub-bands for the transport calculation. The matrix element of the Hamiltonian between the α^{th} atom within the n^{th} slab and the β^{th} atom within the m^{th} slab is given as follows

$$H_{n\alpha,m\beta} = H^0_{n\alpha,m\beta} + \delta_{n\alpha,m\beta} U_{n\alpha} \quad (1)$$

The quantum confinement of the carriers in one dimension opens up the band gap and reduces the electron velocity and the band linearity near the Dirac point. The non-linearity is corrected for each sub-band using effective mass model given by

$$\left[E_b(k) - \frac{E_g^b}{2} \right] \left[\frac{1}{2} + \frac{E_b(k)}{E_g^b} \right] = \frac{\hbar^2 k^2}{2m_b^*} \quad (2)$$

- Step2:** Considering the initial potential distribution, the energies and the wave-function for the sub-band are obtained as a function of longitudinal direction by repeating tight-binding calculation for every slab of the GNR only at $k=0$.
- Step3:** The Hamiltonian matrix, Green's function, contact self-energies and the corresponding level broadening function are obtained for a given sub-band. The transport equations based on the NGEF formulation has a Hamiltonian similar to Tight Binding case. The non-parabolic band diagram is corrected using position-energy dependent effective mass model given as

$$m_b(x, E) = \begin{cases} m_b^* \left[1 + \frac{E - E_c^b(x)}{E_g^b(x)} \right] & \text{if } E > E_i^b(x) \\ m_b^* \left[1 + \frac{E_v^b(x) - E}{E_g^b(x)} \right] & \text{if } E < E_i^b(x) \end{cases} \quad (3)$$

The retarded Green's function is constructed based on the obtained Hamiltonian.

$$G_b(E) = \left[EI - H_b - \sum_s^b - \sum_D^b \right]^{-1} \quad (4)$$

Before the GNR channel is connected to drain and source contacts, the DOS (Density of States) of GNR channel consists of sharp levels at the sub-band minimum energies due to quantum confinement. At the same time, there is a continuous distribution of states in source and drain contacts. Coupling of discretized and continuous states results in a spread of states from channel to contacts and vice-versa over a range of energies. The level broadening quantities are calculated as

$$\begin{aligned} \Gamma_s^b &= i(\sum_s^b - \sum_s^{b+}) \\ \Gamma_D^b &= i(\sum_D^b - \sum_D^{b+}) \end{aligned} \quad (5)$$

- Step 4:** Calculation of source and drain correlation functions and the corresponding electron and hole numbers.

$$\begin{aligned} G_b^<(E) &= G_b(E) \left[\sum_s^{b<} (E) + \sum_D^{b<} (E) \right] G_b^+(E) \\ G_b^>(E) &= G_b(E) \left[\sum_s^{b>} (E) + \sum_D^{b>} (E) \right] G_b^+(E) \end{aligned} \quad (6)$$

$$\sum_{S/D}^{b<} (E) = i \Gamma_{S/D}^b f_{S/D}(E) \quad (7)$$

$$\sum_{S/D}^{b>} (E) = i \Gamma_{S/D}^b [1 - f_{S/D}(E)] \quad (8)$$

$$f_{S/D}(E) = \left[1 + \exp \left(\frac{E - E_{F_{S/D}}}{k_B T} \right) \right]^{-1} \quad (9)$$

The electron and hole numbers at (n, α) atom site is achieved from

$$n_{n\alpha} = -2i \sum_b [|\varphi_{n\alpha}^b|^2 \int_{E_i^b(x)}^{\infty} \frac{1}{2\pi} G_b^<(n, n; E) dE] \quad (10)$$

$$P_{n\alpha} = 2i \sum_b [|\varphi_{n\alpha}^b|^2 \int_{-\infty}^{E_i^b(x)} \frac{1}{2\pi} G_b^>(n, n; E) dE] \quad (11)$$

- Step 5:** Computation of new potential energy using the electron and hole numbers using the Poisson Equation. The 3D Poisson equation is as follows

$$\nabla \cdot [\epsilon(\vec{r}) \nabla U_{n\alpha}(\vec{r})] = qQ(\vec{r}) \quad (12)$$

- Step 6:** Computation of drain current using the Transmission Function $T(E)$.

$$I_{DS} = \frac{2q}{h} \int_{-\infty}^{\infty} T(E) [f_s(E) - f_D(E)] dE \quad (13)$$

$$T_b(E) = \text{Trace}[\Gamma_s^b G_b \Gamma_D^b G_b^+] \quad (14)$$

A. GNRFET Structure

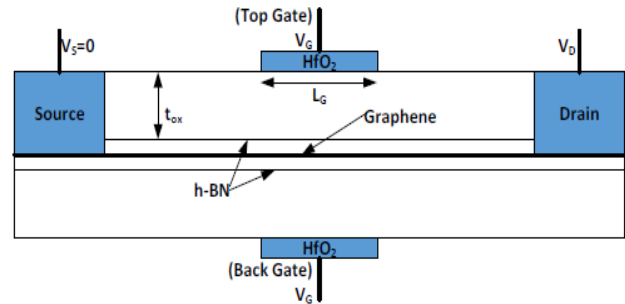


Figure 4: Double gate GNRFET structure

The double gate GNRFET structure is shown in **Figure 4**. The GNR is sandwiched between two insulator layers in double metal gate topology. This provides maximal electrostatic control of the gate electrode over the GNR channel. A h-BN layer is used as a buffer layer, which results in high- k gate insulator free from trapped impurities. The proposed device has HfO_2 dielectric layer with relative permittivity $\epsilon_r = 24$ and oxide thickness $t_{ox} = 1.2\text{nm}$. The dielectric permittivity of h-BN layers is $\epsilon_r = 4$ and the interlayer spacing between GNR and h-BN layers is around 0.3nm . A resultant equivalent silicon oxide gate thickness of 0.5nm is obtained. The length of intrinsic GNR channel is 7.5nm and the symmetric regions of GNR channel are heavily doped with concentration of 0.01 n-type dopants per carbon atom and connected to metallic contacts.

III. SIMULATION & RESULTS

The device described in Section II is simulated to obtain drain current under different bias conditions. The full quantum transport model based on NEGF formalism for the GNRFET as described in **Figure 2** and **Figure 3** is modeled and simulated in MATLAB.

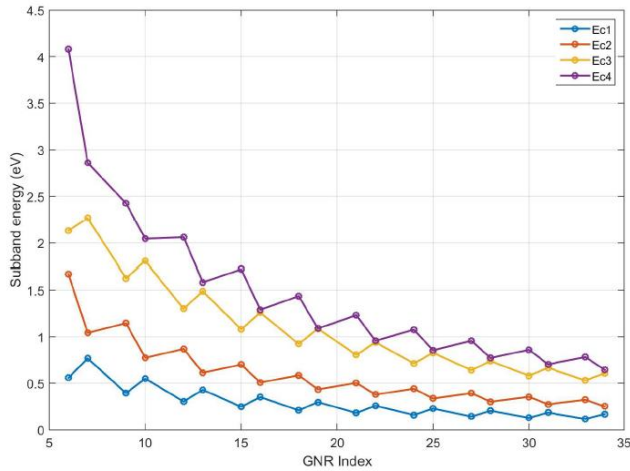


Figure 5: Sub-band energies for different GNR indices

Figure 5 shows the sub-band energies of the GNRFET for different values of the GNR index. The width of the GNR FET is also proportional to the GNR index. The $(3p+1,0)$ GNR family has a higher bandgap than the $(3p,0)$ family. The second sub band can significantly contribute to carrier transport, as its energy is very close to the first sub band energy.

Figure 6 and **Figure 7** shows the transfer characteristics I_{DS} - V_{DS} for the GNRFET for $(3p,0)$ and $(3p+1,0)$ family respectively. The device shows a good MOSFET type behavior which is evident from the strong saturation region. The saturation slope depends on GNR width. Increasing V_{DS} in a wider GNRFET significantly increases the depletion of electrons in the valence band corresponding to hole accumulation in GNR channel.

The transfer characteristics I_D - V_{GS} for GNR $(3p,0)$ family and GNR $(3p+1,0)$ family are given in **Figure 8** and **Figure 9**. As the GNR width increases, the transfer curve shifts towards the lower gate voltages thereby reducing the threshold voltage. Hence, a wide channel GNRFET shall have a lower threshold voltage. At the same time, comparing the two families of GNRFETs, the $(3p,0)$ family has a higher drain current and lower threshold voltage than the $(3p+1,0)$ family. As a result of smaller bandgap and higher number of conducting sub-bands available at a given bias condition, the ON and OFF currents are increased by increasing the GNR width. **Error! Reference source not found.** shows the drain current for gate and drain biases for GNR $(13,0)$.

Figure 10 shows the local density of states for GNRFET for GNR $(12,0)$. The local density of states for GNR $(24,0)$ is shown in **Figure 11**. Comparing the two figures, it is seen that the energy gap between the valence and the conduction bands is significantly reduced as the GNR width increases. Thermionic transport of electrons with energies higher than the potential barriers is the main contributor to drain current. However, with the increase in the width of GNRs, the band to band tunneling of electrons increases because of reduction in the band gap and also lowering of the effective

mass of electrons. This results in a higher off-state current for GNRs with higher widths.

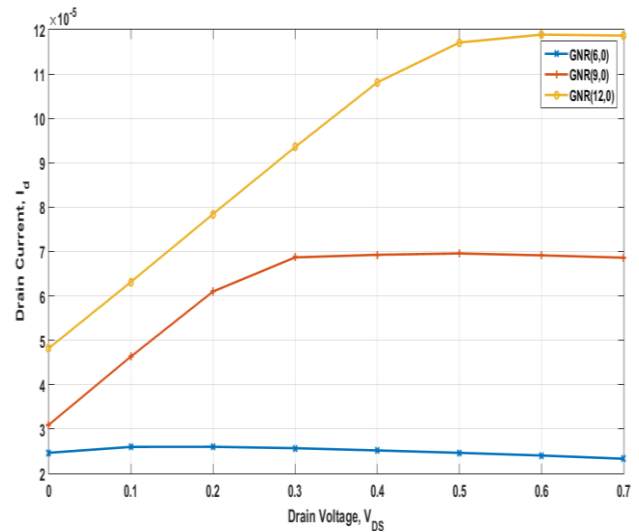


Figure 6: I_D - V_{DS} characteristics for GNR(3p) family

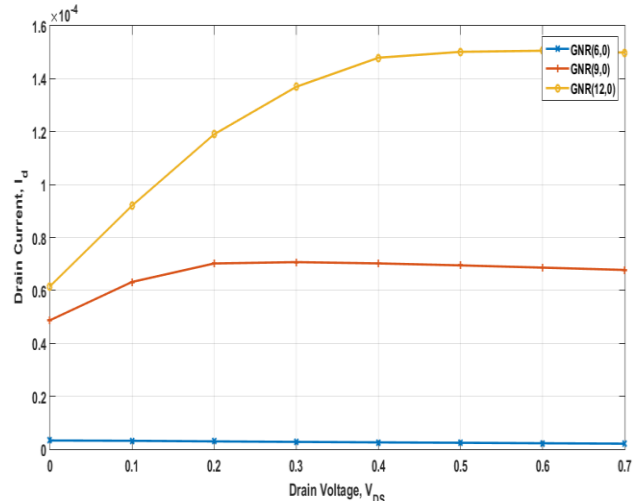


Figure 7: I_D - V_{DS} characteristics for GNR(3p+1) family

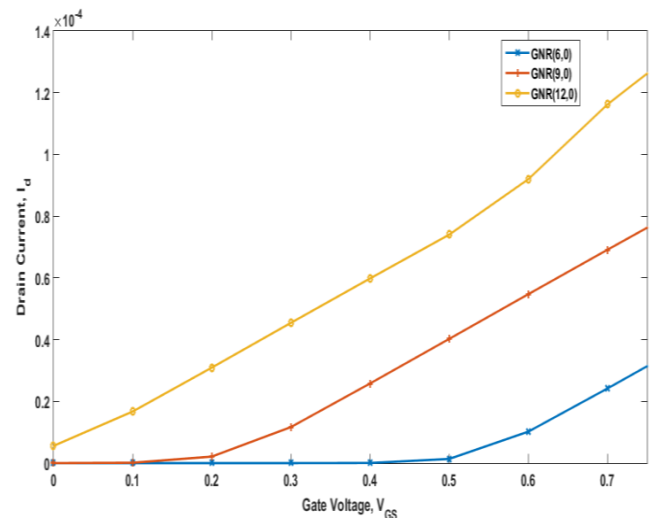


Figure 8: I_D - V_{GS} characteristics for GNR(3p) family

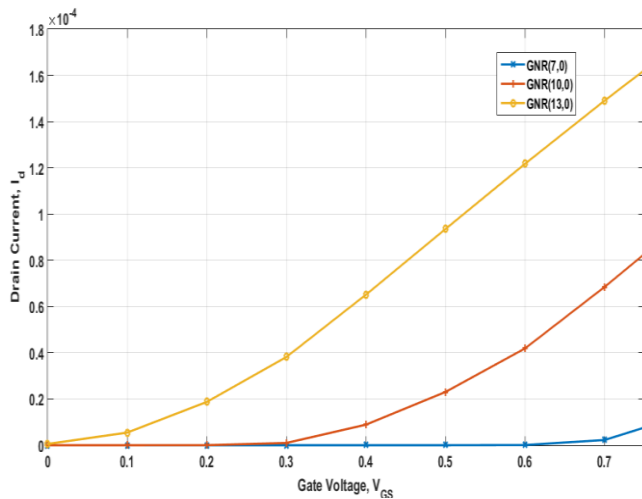


Figure 9: I_D - V_{GS} characteristics for GNR(3p+1) family

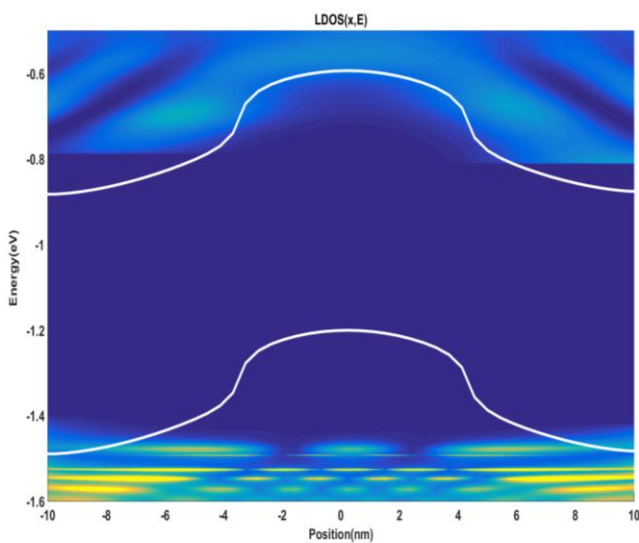


Figure 10: Local density of states calculated using NPEM model for GNR(12,0)

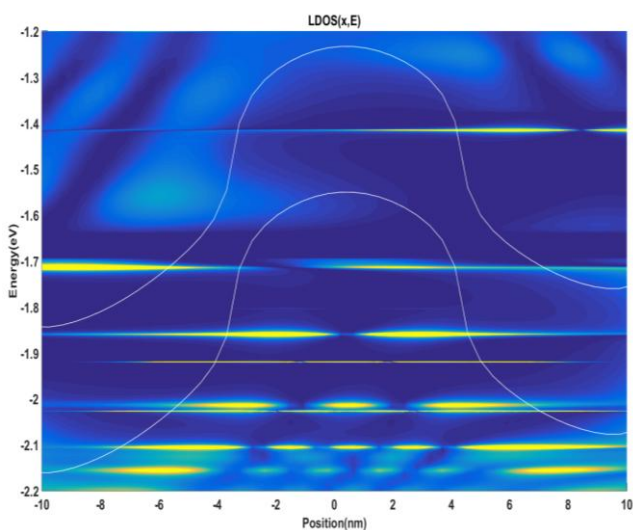


Figure 11: Local density of states calculated using NPEM model for GNR(24,0)

IV. CONCLUSION

Transistor fabrication with reduced dimensionality is not experimentally available, device characteristics need to be optimized by modeling and simulations. Quantum tunneling on carrier transport in sub-10nm devices can be captured by using quantum mechanics based modeling and simulation, wherein short gate length electrostatic effects, quantum tunneling effects can be effectively treated. NGEF approach is an accurate quantum based method for bottom up simulation. This paper presents a fast numerical algorithm based on NGEF formulation for the evaluation of width dependent graphene nanoribbon double gate GNRFET with high-k dielectrics.

A double gate GNRFET is simulated by solving quantum transport equation with self-consistent electrostatics in mode space, while incorporating non-parabolic band structure of GNRFET. This paper provides an investigation and optimization of GNR width. Increasing the GNR width improves the on-state device performance. An investigation of the static attributes of GNRFETs is carried out for two families of armchair GNRs (3p,0) and (3p+1,0). GNR(3p,0) has a smaller bandgap and effective mass, leading to a superior on-state performance.

Investigation of device characteristics for dependence on GNR width reveals the potential benefits of GNRFET and also its limitations for future applications in VLSI. Width dependent GNRFET with wider GNR channel shows better on-state performance by scaling the channel length and supply voltage, indicating a more preferable behavior for lowpower IC design. Increasing the GNR width improves the ON-state performance to some extent by increasing the band-to-band tunneling of electrons from valence band in channel to empty states in the drain region.

REFERENCES

1. "International technology roadmap for semiconductors (ITRS)", <http://www.itrs.net/>, 2013.
2. R. Van Noorden, "Moving towards a graphene world", Nature, vol. 442, no. 7100, pp.228-229, 2006.
3. A. H. C. Neto, "The carbon new age", Materials Today, vol. 13, no. 3, pp. 12-17, 2010.
4. K. Kim, J.-Y. Choi, T. Kim, S.-H. Cho, and H.-J. Chung, "A role for graphene in siliconbased semiconductor devices", Nature, vol. 479, no. 7373, pp. 338-344, 2011.
5. K. S. Novoselov, V. Fal, L. Colombo, P. Gellert, M. Schwab, and K. Kim, "A roadmap for graphene", Nature, vol. 490, no. 7419, pp. 192-200, 2012.
6. Y. Obeng, S. De Gendt, P. Srinivasan, D. Misra, H. Iwai, Z. Karim, D. Hess, and H. Grebel, "Graphene and emerging materials for post-CMOS applications", 215th ECS Meeting, pp. 1-12, 2009.
7. X. Li, W. Cai, J. An, S. Kim, J. Nah, D. Yang, R. Piner, A. Velamakanni, I. Jung, and E. Tutuc, "Large-area synthesis of high-quality and uniform graphene films on copper foils", Science, vol. 324, no. 5932, pp. 1312-1314, 2009.
8. I. Meric, M. Y. Han, A. F. Young, B. Ozyilmaz, P. Kim, and K. L. Shepard, "Current saturation in zero-bandgap, top-gated graphene field-effect transistors", Nature Nanotechnology, vol. 3, no. 11, pp. 654-659, 2008.
9. Y. Ouyang, Y. Yoon, and J. Guo, "Scaling behaviors of graphene nanoribbon FETs: A three-dimensional quantum simulation study", IEEE Transactions on Electron Devices, vol. 54, no. 9, pp. 2223-2231, 2007.
10. X. Guan, M. Zhang, Q. Liu, and Z. Yu, "Simulation investigation of double-gate CNRMOSFETs with a fully self-consistent NEGF and TB method", IEDM Tech. Dig. vol.761, p. 764, 2007.

11. G. Liang, N. Neophytou, M. S. Lundstrom, and D. E. Nikonov, "Ballistic graphene nanoribbon metal-oxide-semiconductor field-effect transistors: A full real-space quantum transport simulation", *Journal of Applied Physics*, vol. 102, no. 5, p. 054307, 2007.
12. R. Grassi, A. Gnudi, E. Gnani, S. Reggiani, and G. Baccarani, "Mode space approach for tight binding transport simulation in graphene nanoribbon FETs", *IEEE Transactions on Nanotechnology*, vol. 10, no. 3, pp. 371-378, 2011.
13. A. Javey, J. Guo, Q. Wang, M. Lundstrom, and H. Dai, "Ballistic carbon nanotube field-effect transistors", *Nature*, vol. 424, no. 6949, pp. 654-657, 2003.
14. Y. M. Banadaki, S. Sharifi, and A. Srivastava, "Investigation of chirality dependence of carbon nanotube-based ring oscillator", *IEEE 58th International Midwest Symposium on Circuits and Systems (MWSCAS)*, pp. 924-927, 2015.
15. A. Martinez, M. Bescond, J. R. Barker, A. Svizhenko, M. Anantram, C. Millar, and A. Asenov, "A self-consistent full 3-D real-space NEGF simulator for studying nonperturbative effects in nano-MOSFETs", *IEEE Transactions on Electron Devices*, vol. 54, no. 9, pp. 2213-2222, 2007.
16. G. Fiori, and G. Iannaccone, "Simulation of graphene nanoribbon field-effect transistors", *IEEE Electron Device Letters*, vol. 28, no. 8, pp. 760-762, 2007.
17. Y. M. Banadaki, and A. Srivastava, "Investigation of the width-dependent static characteristics of graphene nanoribbon field effect transistors using non-parabolic quantum-based model", *Solid-State Electronics*, vol. 54, no. 4, pp. 462-467, 2015.
18. G. S. Kliros, "Gate capacitance modeling and width-dependent performance of graphene nanoribbon transistors", *Microelectronic Engineering*, vol. 112, pp. 220-226, 2013.

AUTHORS PROFILE



Nanda B.S., received her B E in E & C Engineering from P E S college of Engineering(PESCE), Mandya, University of Mysore and M.Tech in Industrial Electronics from SJCE Mysore, VTU Belgavi. She is currently working as Associate Professor in E& C Engg department, PESCE,

Mandya. She is presently pursuing Ph. D in nano-electronics.



Dr. P S Puttaswamy, received his Bachelor Engineering in Electrical Power from University of Mysore in 1983, Master of Engineering and P.hD in Power Apparatus and Electric Drives from University of Roorkee in 1989 and 2000 respectively. After graduated he joined as a Lecturer in PES College of Engineering, Mandya. Since then he worked in PES

College of Engineering, Mandya as Senior Lecturer, Assistant Professor, Professor and Head of the Department of Electrical and Electronics Engineering, Mandya. His areas of Research interests are Power Electronics, Solid State Drives Control, Power System Stability Enhancement using FACTS Controller, Power Quality assessment and their Mitigation and Image Processing techniques.